Adsorbed or intercalated: Na on graphene/Ir(111)

Petar Pervan[1,*] and Predrag Lazić[2,†]
[1]*Institute of Physics, Bijenička 46, HR-10000 Zagreb, Croatia*
[2]*Rudjer Boskovic Institute, Bijenička 54, HR-10000 Zagreb, Croatia*
(Received 21 June 2017; published 7 September 2017)

Interaction of sodium with graphene (Gr) on Ir(111) was studied with the aim to resolve the issue of Na adsorption/intercalation kinetics. The system Na/Gr/Ir(111) was studied by means of angle-resolved photoemission spectroscopy, low-energy electron diffraction, and *ab initio* density functional theory (DFT) calculation. It has been found that at room temperature (RT) and low concentrations Na is dominantly adsorbed on graphene. At higher concentrations, an intercalation process sets in so that it is possible to observe the coexistence of these two states. Eventually, all Na atoms are found in the intercalated state as determined by exposure to oxygen. While adsorption of Na on graphene already intercalated by Na [Na/Gr/Na/Ir(111) system] at RT was not possible, we could observe Li adsorption through the increase of Dirac point binding energy. Li coadsorption strongly affects the binding energy of the iridium surface state as well. This finding was supported by DFT calculations of adsorption energy of Na and Li on bare and fully Na intercalated graphene.

DOI: 10.1103/PhysRevMaterials.1.044202

I. INTRODUCTION

Despite the extraordinary physical properties of graphene, there are several reasons why, from the early days of graphene research, scientists have been trying to alter its structural and electronic properties [1] as well as its interaction with the supporting surfaces [2–4]. Chemical functionalization of graphene was widely used in order to tune its electronic properties [5,6] and to introduce a band gap at the Fermi level [1,3,7]. In the same vein, it has been demonstrated that adsorption and/or intercalation of alkali metals (AMs) could be successfully used to modify the charge-carrier density in graphene, manipulate its electronic structure [8,9], and thereby alter its chemical reactivity [10–12].

In some cases, AM adsorption/intercalation results in electron transfer to graphene without any significant alteration of its electronic structure [13,14]. The outcome of such AM application is reportedly a virtually rigid shift of the graphene π bands [15]. By contrast, some other systems show a clear departure from the rigid band shift [16]. Also, the intercalation of graphene by AMs is known to alter its collective electronic properties [9,14,17,18]. A doping-induced shift of the Dirac point to higher binding energies is usually associated with the band renormalization just below the Fermi level which, in turn, is due to the electron-phonon coupling (EPC) [16,19]. The EPC enhancement is expected to induce the superconductive state [17,20,21], as it has been realized for many other carbon-based materials [22]. The unique electronic structure of graphene appears to be very sensitive to its coupling to the substrate to the point of total extinction of characteristic Dirac-like dispersion of π bands around the K point. Coupling to the surface is particularly strong for graphene on Ni [23], Co [24], and Ru [25]. Intercalation of AM can lead to a large increase in the graphene/substrate separation with the effect of graphene decoupling from the substrate accompanied by the recovery of the π band's dispersion [2,26–28].

It is known from the previous extensive research on graphite [29–32] that intercalation of graphene as one of several carbon allotropes is by no means a straightforward process. Graphene with a densely structured two-dimensional mesh appears to be impenetrable for almost all atoms, including hydrogen [33]. Whether particular atoms deposited on graphene will intercalate or not depends on many factors such as intercalation vs adsorption bonding energy, temperature, graphene microstructure (i.e., the existence of wrinkles), etc. [34,35].

While the density functional theory (DFT) calculations almost unanimously indicate that intercalation is an energetically preferable state for all AM atoms with respect to adsorption on graphene [36], the experimental evidence shows a more complex picture [16]. A recent DFT study of AM adsorption/intercalation on graphene supported by the Au/Ni(111) substrate showed a substantially larger binding energy of all AM in the intercalated state than in the adsorbed state [36]. Li apparently has the strongest affinity for intercalation against adsorption with an energy difference of around 1 eV [36]. On the other hand, x-ray photoemission spectroscopy and angle-resolved photoemission spectroscopy (ARPES) study of the AM position with respect to graphene (adsorption vs intercalation) on a one-monolayer (ML) Au/Ni(111) substrate implies that only K and Ca intercalate into the Gr/Au interface, whereas Cs, Rb, Na, and Li adsorb preferably on top of the graphene layer [16]. This result extends the earlier finding of easy intercalation of graphene on Au/Ni(111) by K reported by Varykhalov *et al.* [3] as well.

In contrast to the 1-ML Au/Ni(111) substrate, it seems that graphene on other substrate surfaces (metallic and SiC) is readily intercalated by Li [37–39]. Potassium showed a similar behavior regarding the intercalation of graphene on Ir(111) [19,40,41] and Ni(111) [4,42] at the room temperature (RT).

*pervan@ifs.hr
†plazic@irb.hr

It appears that Cs intercalates graphene on Ni(111) [42] and Ir (111) [35] surfaces at RT as well. However, a combined scanning tunnel microscopy (STM), low electron energy microscopy, and ARPES study of Cs intercalation of graphene on Ir(111) has shown that the process follows a somewhat more complicated path [35]. At submonolayer coverages, Cs displays the coexistence of adsorbed and intercalated phases (see Fig. 2 in Ref. [35]) such that the intercalation process is in a delicate energetic balance relative to adsorption, which is due to van der Waals interaction between graphene and the iridium surface. Although this has not been explicitly discussed, it appears as if K interaction with Gr/Ir(111) exhibits a similar coexistence of adsorbed and intercalated phases [see Fig. 2(a) in Ref. [40]] at the initial K coverage.

Sodium appears to be an exception when it comes to AM intercalation of graphite; that is, it is the only AM that does not intercalate [32,43]. Different aspects of Na intercalation of graphene on metal surfaces are still being debated. Park *et al.* [26] reported a complete recovery of the electronic structure of graphene from the strongly interacting Ni surface by spontaneous Na intercalation at RT. Even more recent experiments by Matyba *et al.* [2] have convincingly demonstrated that Na adsorbs preferably on graphene on Ni(111) at RT and that intercalation takes place only at elevated temperatures. This is explained in terms of the increased mobility of Na atoms, suggesting that the diffusion of adsorbed Na from the external graphene surface to the intercalated configuration is controlled by kinetic effects, e.g., penetration through graphene defects (i.e., the wrinkles at grain boundaries) [35].

STM and ARPES investigations of Na interaction with graphene on Ir(111) imply that Na does not intercalate but rather remains adsorbed; initially, it decorates the step edges, whereas at higher coverages it forms single-layer islands [7]. Such an adsorbed layer of Na was reported to downshift the Dirac point to 1.5 eV below the Fermi level. On the other hand, Gall *et al.* [44] have found that Na, and likewise K and Cs, intercalates graphene on Ir(111) in the temperature interval 300–700 K, as verified by Auger electron spectroscopy and thermal desorption spectroscopy. Finally, Langer *et al.* [45] concluded in their study of sheet plasmons in bare and Na intercalated graphene on Ir(111) that Na intercalates fully at RT.

The aim of this work is to contribute to the resolution of the dilemma over Na adsorption vs intercalation of graphene (Gr) on Ir(111) through a detailed ARPES and DFT study of this system. We show that, initially, Na preferentially adsorbs on Gr/Ir(111) at RT, but with further exposure, we observe signatures of Na intercalation. Finally, after long exposures all the Na atoms become intercalated, and no indications of adsorbed Na were found. Moreover, we are able to demonstrate that the large shift of the Dirac point to higher binding energies is associated with intercalation and not with an adsorbed state of Na atoms. We also show that once the graphene layer is intercalated by Na, no extra Na adsorption on top of graphene is possible, while Li adsorption (under the same conditions) proves possible, leading to an additional charge transfer to graphene and to a further shift of the Dirac point to higher binding energies. The experiments were corroborated by the DFT calculations of adsorption energies of Na and Li on bare and intercalated graphene.

II. EXPERIMENTAL AND COMPUTATIONAL DETAILS

Experiments were performed in an ultrahigh-vacuum ARPES facility. The ARPES spectra were recorded by a Scienta SES100 hemispherical electron analyzer with an overall energy resolution of 25 meV and an angular resolution of 0.2°. Photons of 21.2 eV from a nonpolarized He-discharge ultraviolet source (beam-spot diameter of around 2 mm) were used for excitation.

An iridium single crystal of 99.99% purity and orientation accuracy better than 0.1° was used. The substrate was cleaned by several cycles of sputtering with 1.5 keV Ar^+ ions at room or elevated temperature (1100 K) followed by annealing at 1500–1600 K. The cleanliness and quality of Ir(111) were checked by low-energy electron diffraction and ARPES (surface-state sharpness and intensity [46]). The graphene monolayer on Ir(111) was prepared by a temperature-programmed growth cycle (TPG; room-temperature ethene exposure 6×10^{-6} Pa for 60 s and flash to 1400 K) followed by chemical vapor deposition (CVD; 6×10^{-6} Pa of ethene for 300 s while the sample was held at 1150 K). This TPG + CVD procedure growth leads to uniform orientation of graphene with the lattice aligned to the substrate lattice (R0) and at full monolayer coverage [47]. Sodium was deposited from a commercial getter source while the sample surface was kept at room temperature. The extremely reactive sodium adatoms, particularly at higher coverages when a metallic layer is formed, are susceptible to contamination from the residual gas molecules [10,48]. The experiments were prepared and performed by taking all the necessary steps to ensure that the experimental results were not affected by undesired adsorption; that is, they were carried out at low base pressure during Na deposition and data acquisition.

Ab initio calculations were performed within the framework of DFT [49,50] as implemented in the VASP code [51,52] with the projector augmented-wave method [53,54]. We used a self-consistently implemented van der Waals density functional (vdW-DF) [55,56] for correlation in combination with the optimized Becke88 (optB88) for the exchange energy [57]. The lattice constant of the Ir bulk was determined self-consistently, while the graphene lattice constant was adjusted to match the Ir(111) surface lattice constant, resulting in some strain (∼10%) on the graphene. This makes graphene somewhat more reactive in binding to Li and Na. However, the relative strength of the binding is still correct.

In all calculations, the expansion in plane waves was done using the cutoff energy of 500 eV. The Brillouin zone was sampled by a Monkhorst-Pack [58] choice of $3 \times 3 \times 1$ k points. The Ir(111) surface slab was simulated by five atomic layers, of which the top two, along with the C and Li/Na atoms, were allowed to relax until the forces on atoms were below 1 meV/Å. In all calculations, the size of the surface unit cell was 4×4 (for Ir unit cells, the graphene unit cell was expanded by about 10% to fit commensurably). Such a structure accommodates a maximum of 16 intercalated and 16 adsorbed Li/Na atoms. Different coverages were simulated by randomly distributing a selected number of Li/Na atoms. Dipole correction [59,60] in the direction perpendicular to the slab was used with 20 Å of vacuum separating the periodic slab images.

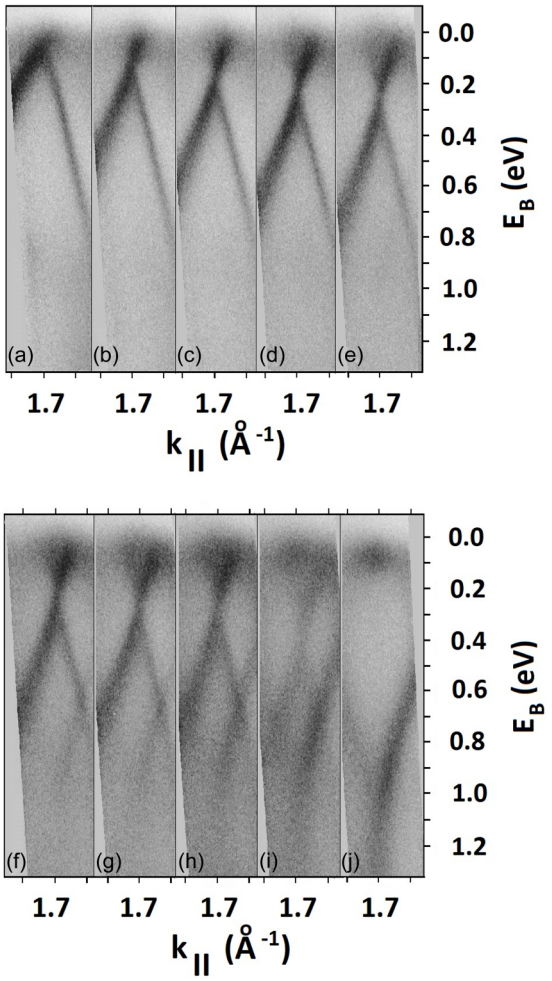

FIG. 1. ARPES spectra of Gr/Ir(111) around the K point along Γ-K-M as a function of Na deposition time (see the text).

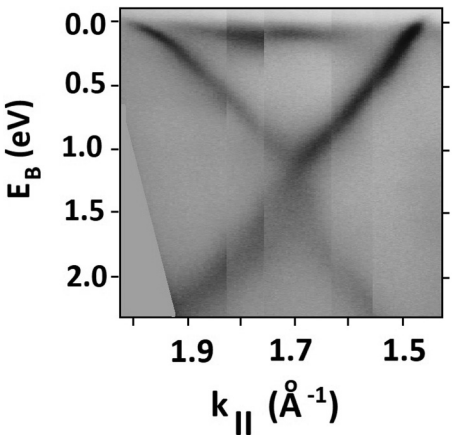

FIG. 2. ARPES spectra of Gr/Ir(111) around the K point along Γ-K-M for the Na saturation coverage.

III. RESULTS AND DISCUSSION

The high quality of prepared graphene was, prior to sodium exposure, judged by the spectral linewidth of graphene π bands (see Fig. 4 in Ref. [47]). The current through the Na dispenser was adjusted to ensure a low deposition rate in order to capture any possible change in the graphene band structure during Na adsorption/intercalation. Figure 1 shows the dispersion of graphene π bands in a narrow momentum window around the K point as a function of Na deposition time. As expected, due to electron doping, Na induces a shift of the Dirac point to higher binding energy which saturates after 20 min at an energy of around 0.3 eV [see Fig. 1(f)]. Further deposition (29 min) does not affect the Dirac point or the shape of the Dirac cone. However, more Na deposition does induce changes in the whole spectrum in the form of an additional graphene π band [see Fig. 1(g)]. As the exposure time increases, a pattern of the second Dirac cone becomes more discernible, while the intensity of the first Dirac cone is eventually completely reduced. The spectrum after 120 min of Na exposure [Fig. 1(j)] exhibits graphene π bands with the Dirac point around 1.2 eV. There also appears to be some intensity at the Fermi level which is associated with the iridium surface state [47].

When the new Dirac cone emerges, further exposure to Na induces a steady shift of the Dirac point to higher binding energies such that for the Na saturation coverage the Dirac point reaches an energy of around 1.3 eV (see Fig. 2), which is somewhat smaller than observed previously [7]. At the saturation coverage, we could not observe any Na-induced superstructure. This result is consistent with the observation of Papagno *et al.* [7], who were not able to detect any Na-induced superstructure in their STM images either. They concluded that Na saturation coverage was most likely consistent with the (2×2) periodicity [7] corresponding to $\Theta_{Na} = 0.125$ with respect to graphene. ARPES maps shown in Figs. 1(h) and 1(i) are very similar to the spectrum observed for Cs/Gr/Ir(111), which showed the coexistence of adsorbed and intercalated phases of Cs [35]. Based on this simple analogy, we can put forward a hypothesis that the spectra with the Dirac point at 0.3 and 1.3 eV below the Fermi level correspond to the adsorbed and intercalated phases, respectively. This assumption is clearly in contradiction to the conclusion of Papagno *et al.* [7], who found that the band structure of graphene saturated by Na with the Dirac cone at 1.5 eV was associated with the Na atoms adsorbed on top of graphene. In order to resolve whether our ARPES spectrum of strongly n doped graphene corresponds to either adsorbed or intercalated graphene, we performed an oxygen exposure experiment. Matyaba *et al.* [2] unambiguously demonstrated that intercalated Na is protected from oxidation by graphene so that extended exposure to oxygen does not affect the ARPES spectrum. However, when Na atoms are adsorbed on top of graphene the exposure to oxygen dramatically changes the valence-band spectrum around the K point. Instead of the graphene π bands, two nondispersing states related to sodium oxides emerged (see Fig. S3 in Ref. [2]). As Fig. 3 suggests, after exposure of Gr/Na/Ir(111) to 100 L of oxygen, no change in the valence-band structure around the K point was observed either. Figure 3 shows a portion of the graphene spectrum around $k_F \approx 1.45\,\text{Å}^{-1}$. Any shift of the Dirac point towards the Fermi level (due to the oxidation of the Na layer) would lead to, as a consequence, a decrease in the Fermi surface, i.e., a shift of k_F closer to the K point. The change in k_F is negligibly small, indicating that Na was protected by the

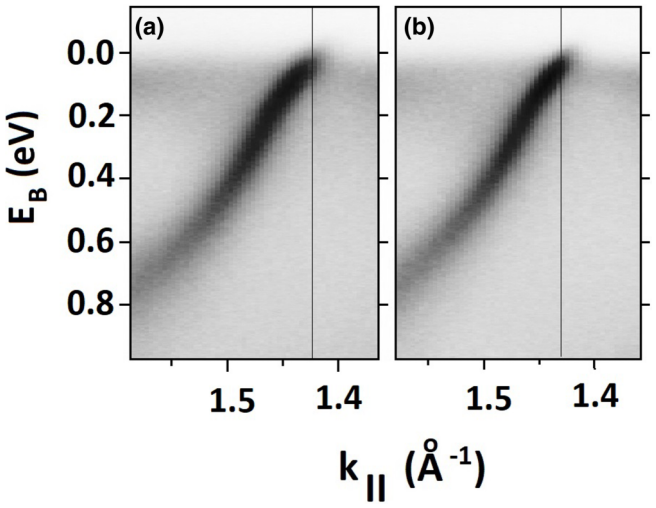

FIG. 3. ARPES spectrum of the Γ-K-M branch of Gr/Na/Ir(111) (a) prior to and (b) after exposure to 100 L of oxygen.

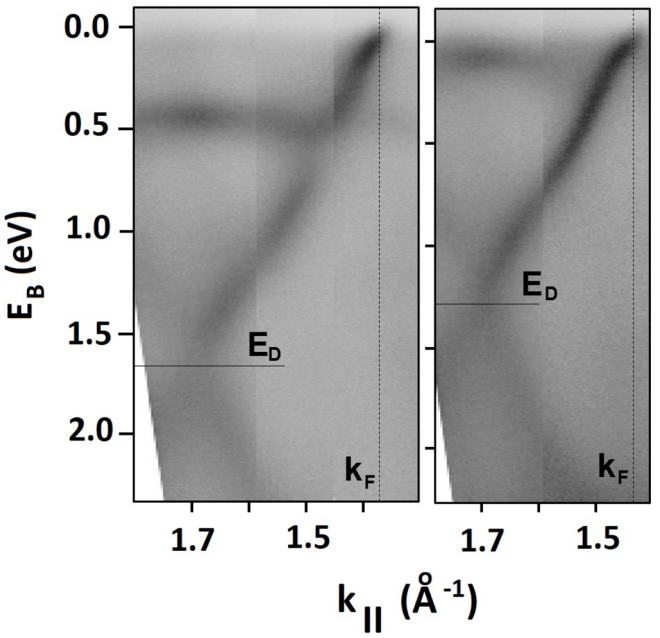

FIG. 4. ARPES spectrum of Li/Gr/Na/Ir(111) along Γ-K-M before (left) and after (right) oxygen exposure (100 L).

graphene mesh. From these results, we draw the conclusion that the ARPES spectrum shown in Fig. 2 corresponds to Na intercalated between graphene and the Ir surface.

After completion of the Na-intercalated layer any attempt to adsorb more Na on top of graphene failed as additional exposure to Na introduced no change in the valence-band spectrum. However, we did see a noticeable change in the spectrum if the Gr/Na/Ir(111) sample was exposed to Li instead. In the following, we shall demonstrate that the deposited Li is not intercalated but adsorbed on top of the Gr/Na/Ir(111) system. The exposure to Li induces a significant shift in the Dirac point to even higher binding energies (from 1.3 to 1.7 eV). This is one of the largest binding energies measured for any doped graphene system [see Fig. 4(a)]. In addition to the shift of the Dirac point, there is a substantial shift of the Ir surface state. The same effect was recently reported for graphene on Ir(111) intercalated by only Li [38]. Instead of quenching the surface state, as some other intercalated atoms do [61], Li atoms placed between graphene and the Ir(111) surface only increase their binding energy without affecting the coherence around the K point [38]. However, in this case the surface state shift is not induced by intercalated Li but rather by adsorbed Li, although the spectroscopic appearance and the binding energy (around 0.45 eV) are the same. The oxygen test was again applied in order to test the Li position with respect to graphene.

As can be seen in Fig. 4(b), the exposure of the Li/Gr/Na/Ir(111) system induces an almost rigid shift of all the bands towards the Fermi level and, consequently, the decrease of k_F from 1.61 to 1.52 Å^{-1}. This shift clearly suggests that oxygen has retrieved electrons that have been transferred from Li to graphene, thus reducing the n doping of the Gr/Na/Ir(111) system. We are confident that deposited Li is in the adsorbed state and not in the intercalated state because the previous experiments of Gr/Li/Ir(111) exposure to oxygen showed no change in the valence-band spectrum whatsoever. This raises the question of why Li adsorbs on the Gr/Na/Ir(111) system and Na does not. Recently, it was unambiguously demonstrated that Cs and Eu do not adsorb at RT on graphene when it is intercalated by Cs and Eu, respectively [62]. The STM data were corroborated by DFT calculations suggesting a strong reduction of the Cs (Eu) adsorption energy on the order of 1 eV when graphene is intercalated by Cs (Eu). As we shall demonstrate shortly, the fact that Na does not adsorb on Gr/Na/Ir(111) while Li does can be explained in the same fashion, i.e., by the difference in their Na intercalation-induced adsorption energies. However, the reduction of adsorption energy on intercalated graphene might not always be big enough to prevent the coexistence of intercalated and adsorbed states at RT as in the case of K/Gr/K/Ir(111) [40]. As the experiment showed, elevated temperatures (above 360 K) are required in order to suppress K adsorption on Gr/K/Ir(111) [40].

Before discussing the nature of Na and Li bonding to intercalated graphene, we would like to address the observation that Na intercalation does not induce a shift of the Ir surface state below the Fermi level, while Li does [38]. As Fig. 3(b) in Ref. [38] clearly shows, initially, it takes a significant number of Li atoms (i.e., the charge transferred to graphene and the Ir surface) to make a minor shift of the surface state, not larger than 50 meV. It should be noticed that this small shift corresponds to a reduction in the binding energy of the Dirac point as large as 1.3 eV, which is exactly the energy shift observed for graphene intercalated by Na (see Fig. 2). The conclusion is as follows: due to the larger size of Na atoms compared to Li, the saturation coverage of intercalated Na is, in absolute terms, smaller than the saturation coverage of Li. As a consequence, there is a lack of charge transferred to Ir to facilitate the shift of the surface state below the Fermi level. This finding is consistent with the notion that the Na saturation coverage corresponds to a (2×2) superstructure, i.e., $\Theta_{Na} = 0.125$. However, when additional charge is provided by adsorbed Li atoms, the surface state indeed

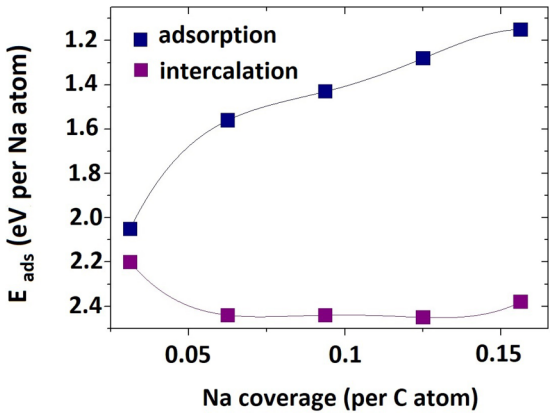

FIG. 5. Calculated adsorption vs intercalation energies for increasing Na coverage. Calculated energy equals the total energy of the system divided by the number of adsorbed/intercalated Na atoms.

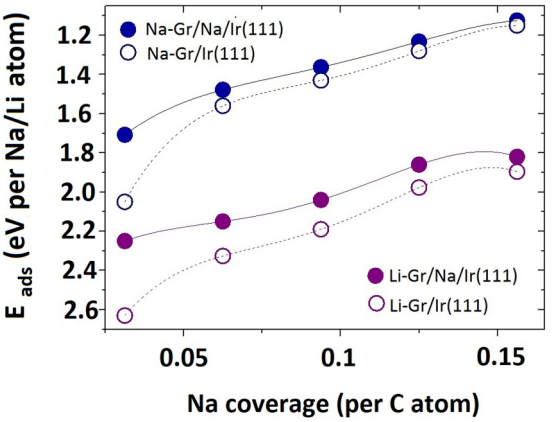

FIG. 6. Calculated adsorption energies of Na and Li on Gr/Na/Ir(111) for increasing Na/Li coverage and saturating Na concentration in the intercalated state. Also shown for comparison are the coverage dependences of adsorption energies of Li and Na on Gr/Ir(111). The lines are to guide the eye.

exhibits a clear departure from the Fermi level. Moreover, due to their larger size Na atoms tend to create a metallic layer at much lower coverages than Li atoms, resulting in the appearance of two-dimensional electron-gas states which can further accommodate Na electrons. This effect significantly reduces the donation of Na electrons to graphene or iridium.

Next, we provide theoretical support for the observed mechanism of Na adsorption/intercalation of graphene on Ir(111). As Fig. 5 shows, initial adsorption of Na on Gr/Ir(111) is just slightly less energetically favorable than intercalation. The calculation of Jin *et al.* [63] also shows that adsorption of two Na atoms on the same side of graphene is energetically less favorable than on opposite sides of the graphene layer (one Na atom on each side), thereby supporting the picture of the intercalation process. However, being initially adsorbed, a Na atom does not experience a particularly strong driving force to change its state from adsorption to intercalation. Yet, as the concentration of adsorbed Na increases, the intercalation becomes significantly energetically more favorable (by around 0.9 eV). At $\Theta_{Na} = 0.125$ the energy difference in favor of intercalation rises to 1.15 eV. Therefore, the increasing coverage of adsorbed Na exerts "pressure" on Na atoms to take the position of higher binding energy, i.e., of the intercalated state. As has been compellingly demonstrated in the case of Cs intercalation of Gr/Ir(111), Cs coverage has to reach a value of 0.1 ML (corresponding to $\Theta_{Cs} \approx 0.03$ per carbon atom) before the channel for intercalation is opened. A similar pattern of coexistence of the AM adsorbed and intercalated states that precedes fully intercalated graphene was recently reported for K/Gr/Ir(111) [40]. Judging from the coverage dependence of Na adsorption vs intercalation energy (see Fig. 5), we estimate that the coverage $\Theta_{Na} \approx 0.05$ is required in this case before intercalation sets in. Notice also that with increasing Na coverage the intercalation energy remains constant while at the same time the adsorption energy experiences a substantial decrease, making the process of intercalation at higher Na coverages even more likely. This widening energy gap between adsorption and intercalated state supports our view that at RT an increased supply of Na atoms on graphene accelerates the intercalation process. It is obvious that the mobility of adsorbed AM on graphene should play an important role in the kinetics of the intercalation process. A repulsive force between induced dipoles of adsorbed AM facilitates the motion of adatoms across graphene in finding their path to underneath graphene [35]. However, since this is an activated process, it is not surprising that the surface temperature can have a decisive impact on the mobility and, ultimately, on the intercalation of AM adatoms. It has been shown that adsorption of K on Gr/Ir(111) at 80 K freezes out the intercalation process entirely, and only the annealing at RT and higher (up to 360 K) provides K adatoms with large enough mobility to promote intercalation [40].

Figure 6 shows the concentration dependence of the Na(Li) adsorption energy on graphene that was previously intercalated by Na. Note that the adsorption energy of an isolated Na atom on intercalated graphene [$E_{\text{ads}}(\text{I}) = 1.75$ eV] is reduced by 0.3 eV with respect to nonintercalated graphene [$E_{\text{ads}}(\text{NI}) = 2.05$ eV].We observe that a similar reduction of adsorption energy on intercalated graphene is also experienced by an isolated Li atom. The decrease in adsorption energy upon graphene intercalation is not as large as for Cs or Eu but is obviously large enough to have a similar impact on the adsorption kinetics [62] of Na and Li. We see from Fig. 6 that for all Na and Li concentrations on Gr/Na/Ir(111) lithium atoms exhibit a noticeably larger adsorption energy. Previous theoretical calculations of Li and Na adsorption energies consistently gave significantly larger values for Li relative to Na in the case of unsupported graphene as well as for Gr/Au/Ni(111) (see Table II in Ref. [36]). At this point, it is appropriate to address the nature of the difference of the strength of bonding of Li and Na to graphene. Namely, since Na is a more reactive alkali atom than Li, it should benefit more from charge donation to graphene in ionic bond formation. From that point of view, Na should bond more strongly to graphene than Li. However, due to the small size of the Li atom the charge it donates stays within the Li atomic potential, making the bond with graphene more covalentlike, from which Li benefits by creating a stronger bond. In their analysis of Li^+ and Na^+ interaction with benzene complexes Tsuzuki *et al.* [64] emphasized the significance of the so-called induction

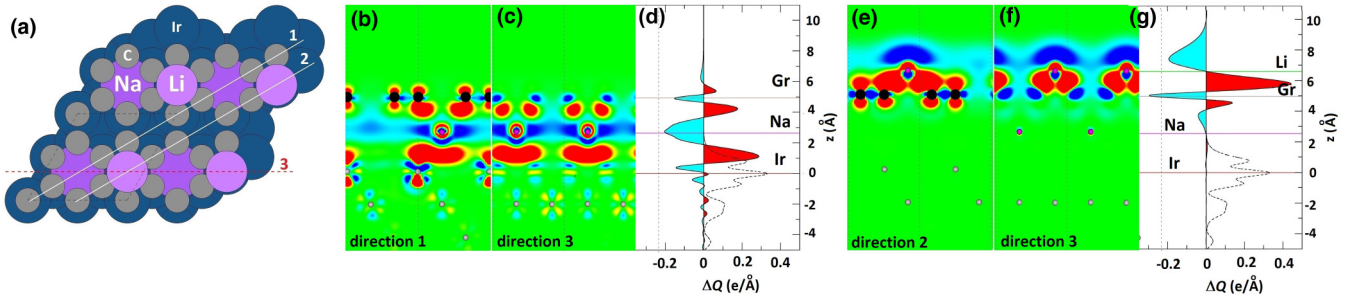

FIG. 7. (a) Structural model of Li/Gr/Na/Ir(111) and Gr/Na/Ir(111) systems indicating three directions along which the calculated charge-transfer density maps are shown in (b) Gr/Na/Ir(111) along direction 1, (c) Gr/Na/Ir(111) along direction 3, (e) Li/Gr/Na/Ir(111) along direction 2, and (f) Li/Gr/Na/Ir(111) along direction 3. (d) and (g) show the corresponding charge rearrangement along the z direction. (d) Charge transfer calculated as the charge difference $Q(\mathrm{Gr/Na/Ir}) - [Q(\mathrm{Gr/Ir}) + Q(\mathrm{Na})]$. (g) Charge transfer calculated as charge difference $Q(\mathrm{Ir/Na/Gr/Li}) - [Q(\mathrm{Ir/Na/Gr}) + Q(\mathrm{Li})]$.

energy which is the interaction energy between the polarizable sites of the benzene complexes and the electric field produced by Li^+ and Na^+. Due to the R^{-4} dependence (R is the distance from the AM cation) of the induction energy, its contribution to Li bonding is more than two times larger than that to Na, making the total bonding energy of Li^+/benzene larger than that of Na^+/benzene [64].

We have also explored within the DFT framework the charge transferred to graphene and iridium upon Na intercalation and additional Li adsorption. Figure 7(a) shows a structural model of a $\mathrm{Li}(2\times2) + \mathrm{Gr/Na}(2\times2)/\mathrm{Ir}(111)$ superstructure with three directions along which the charge-transfer density maps have been calculated. Figures 7(b) and 7(c) show how the charge released by intercalated Na redistributes to Gr and Ir surfaces along directions 1 and 3, respectively. Figure 7(d) displays the corresponding integrated charge rearrangement along the z direction. We see that a significant amount of charge has been transferred from the Na atoms to graphene and Ir. An additional analysis has shown that, likewise, in the case of Li intercalation of graphene [38], the charge transferred from Na to graphene and the Ir surface is almost additive in nature. In other words, the total charge transferred to Gr and Ir through the intercalation is nearly equal to the charge transferred independently from Na to Gr (freestanding Gr) and Ir(111). Additional interesting information arises from the charge-transfer density maps which illustrate how the electronic charge is transferred to Gr and Ir not only from the areas around Na atoms but also from between them. This clearly indicates that at such distances Na atoms are already forming a metallic layer. Figures 7(e) and 7(f) show the calculated charge-transfer density maps of the Li/Gr/Na/Ir(111) systems along directions 2 and 3, respectively. Figure 7(g) displays the corresponding charge rearrangement along the z direction. It is obvious that most of the charge released by Li goes to Gr, while the effect on the Ir surface appears to be reflected merely through the charge redistribution. However, the experimentally observed shift of the Ir surface state upon Li adsorption indicates that there has been some potential change at the interface which induces a shift of the surface state to higher binding energies. Li adsorption charge-transfer density maps [Figs. 7(e) and 7(f)] suggest that apart from the reduction of charge around Li atoms, there is a charge density decrease in between, indicating that for a (2×2) superstructure Li creates a metallic layer as well. This is consistent with DFT calculations by Jin *et al.* [63], who showed that despite the fact that Na and Li exhibit a crossover from an isolated AM to a metallic layer at different coverages, Na and Li should form a metallic layer at the concentration corresponding to the (2×2) superstructure.

To summarize, we have demonstrated that Na initially adsorbs on Gr/Ir(111) at RT but intercalates with continuous exposure. These two states reflect the different electron doping of graphene which is observed through different shifts of the Dirac cone; adsorbed Na induces a shift of the Dirac point to 0.3 eV, while the signature of the fully intercalated Na is the Dirac point at 1.3 eV below the Fermi level. DFT calculations support this scenario, showing that the adsorption of Na is the energetically favorable state relative to intercalation only at low Na concentrations. The increase in Na coverage on the graphene surface significantly reduces adsorption with respect to intercalation energy, building up the pressure for intercalation. This response indicates that the corresponding intercalation kinetics is very similar to that of Cs [35], most likely of K on Gr/Ir(111) [40]. We have also demonstrated that once Na has been intercalated, no additional Na can be adsorbed on graphene at RT, which is explained in terms of reduction of Na adsorption energy upon Na intercalation. However, we have shown that Li does adsorb on Gr/Na/Ir(111) as Li experiences a stronger bonding to graphene than Na. Li adsorption induces a substantial shift of the Ir surface state to higher binding energy, similar to Gr/Li/Ir(111).

ACKNOWLEDGMENTS

We thank B. Gumhalter for useful discussions. P.P. acknowledges the financial support of the Croatian Science Foundation (Grant No. IP-11-2013-2727). P.L. was supported by the Unity through Knowledge Fund, Contract No. 22/15, and Horizon 2020 CSA Twinning Project No. 692194, RBI-T-WINNING.

[1] C. Coletti, C. Riedl, D. S. Lee, B. Krauss, L. Patthey, K. Von Klitzing, J. H. Smet, and U. Starke, Charge neutrality and band-gap tuning of epitaxial graphene on SiC by molecular doping, Phys. Rev. B **81**, 235401 (2010).

[2] P. Matyba, A. Carr, C. Chen, D. L. Miller, G. Peng, S. Mathias, M. Mavrikakis, D. S. Dessau, M. W. Keller, H. C. Kapteyn, and M. Murnane, Controlling the electronic structure of graphene using surface-adsorbate interactions, Phys. Rev. B **92**, 041407 (2015).

[3] A. Varykhalov, M. R. Scholz, T. K. Kim, and O. Rader, Effect of noble-metal contacts on doping and band gap of graphene, Phys. Rev. B **82**, 121101 (2010).

[4] A. Grüneis and D. V. Vyalikh, Tunable hybridization between electronic states of graphene and a metal surface, Phys. Rev. B **77**, 193401 (2008).

[5] D. C. Elias, R. R. Nair, T. M. G. Mohiuddin, S. V Morozov, P. Blake, M. P. Halsall, A. C. Ferrari, D. W. Boukhvalov, M. I. Katsnelson, A. K. Geim, and K. S. Novoselov, Control of graphene's properties by reversible hydrogenation: Evidence for graphane, Science **323**, 610 (2009).

[6] D. Usachov, O. Vilkov, A. Grüneis, D. Haberer, A. Fedorov, V. K. Adamchuk, A. B. Preobrajenski, P. Dudin, A. Barinov, M. Oehzelt, C. Laubschat, and D. V. Vyalikh, Nitrogen-doped graphene: Efficient growth, structure, and electronic properties, Nano Lett. **11**, 5401 (2011).

[7] M. Papagno, S. Rusponi, P. M. Sheverdyaeva, S. Vlaic, M. Etzkorn, D. Pacilé, P. Moras, C. Carbone, and H. Brune, Large band gap opening between graphene Dirac cones induced by Na adsorption onto an Ir superlattice, ACS Nano **6**, 199 (2012).

[8] J. L. McChesney, A. Bostwick, T. Ohta, T. Seyller, K. Horn, J. González, and E. Rotenberg, Extended Van Hove Singularity and Superconducting Instability in Doped Graphene, Phys. Rev. Lett. **104**, 136803 (2010).

[9] A. Bostwick, F. Speck, T. Seyller, K. Horn, M. Polini, R. Asgari, A. H. MacDonald, and E. Rotenberg, Observation of plasmarons in quasi-freestanding doped graphene, Science **328**, 999 (2010).

[10] A. Politano and G. Chiarello, Alkali-induced hydrogenation of epitaxial graphene by water splitting at 100 K, J. Chem. Phys. **138**, 044703 (2013).

[11] S. S. Harilal, J. P. Allain, A. Hassanein, M. R. Hendricks, and M. Nieto-Perez, Reactivity of lithium exposed graphite surface, Appl. Surf. Sci. **255**, 8539 (2009).

[12] B. Heim, C. N. Taylor, and J. P. Allain, Tuning the electronic and chemical surface properties of graphane combining alkali deposition and low-energy ion irradiation, in Nanotechnol. 2010 Adv. Mater. CNTs, Part. Film. Compos. - 2010 NSTI Nanotechnol. Conf. Expo, NSTI-Nanotech 2010, June 21, 2010 - June 24, 2010 (unpublished).

[13] T. Kihlgren, T. Balasubramanian, L. Walldén, and R. Yakimova, K/graphite: Uniform energy shifts of graphite valence states, Surf. Sci. **600**, 1160 (2006).

[14] A. Bostwick, T. Ohta, T. Seyller, K. Horn, and E. Rotenberg, Quasiparticle dynamics in graphene, Nat. Phys. **3**, 36 (2007).

[15] C. G. Hwang, S. Y. Shin, S. M. Choi, N. D. Kim, S. H. Uhm, H. S. Kim, C. C. Hwang, D. Y. Noh, S. H. Jhi, and J. W. Chung, Stability of graphene band structures against an external periodic perturbation: Na on graphene, Phys. Rev. B **79**, 115439 (2009).

[16] V. Fedorov, N. I. Verbitskiy, D. Haberer, C. Struzzi, L. Petaccia, D. Usachov, O. Y. Vilkov, D. V Vyalikh, J. Fink, M. Knupfer, B. Büchner, and A. Grüneis, Observation of a universal donor-dependent vibrational mode in graphene, Nat. Commun. **5**, 3257 (2014).

[17] T. Valla, J. Camacho, Z. H. Pan, A. V. Fedorov, A. C. Walters, C. A. Howard, and M. Ellerby, Anisotropic Electron-Phonon Coupling and Dynamical Nesting on the Graphene Sheets in Superconducting CaC_6 Using Angle-Resolved Photoemission Spectroscopy, Phys. Rev. Lett. **102**, 107007 (2009).

[18] A. Cupolillo, N. Ligato, and L. S. Caputi, Plasmon dispersion in quasi-freestanding graphene on Ni(111), Appl. Phys. Lett. **102**, 111609 (2013).

[19] I. Pletikosić, M. Kralj, M. Milun, and P. Pervan, Finding the bare band: Electron coupling to two phonon modes in potassium-doped graphene on Ir(111), Phys. Rev. B **85**, 155447 (2012).

[20] B. M. Ludbrook, G. Levy, P. Nigge, M. Zonno, M. Schneider, D. J. Dvorak, C. N. Veenstra, S. Zhdanovich, D. Wong, P. Dosanjh, C. Straßer, A. Stöhr, S. Forti, C. R. Ast, U. Starke, and A. Damascelli, Evidence for superconductivity in Li-decorated monolayer graphene, Proc. Natl. Acad. Sci. USA **112**, 11795 (2015).

[21] G. Profeta, M. Calandra, and F. Mauri, Phonon-mediated superconductivity in graphene by lithium deposition, Nat. Phys. **8**, 131 (2012).

[22] A. F. Hebard, M. J. Rosseinsky, R. C. Haddon, D. W. Murphy, S. H. Glarum, T. T. M. Palstra, A. P. Ramirez, and A. R. Kortan, Superconductivity at 18 K in potassium-doped C_{60}, Nature (London) **350**, 600 (1991).

[23] E. Voloshina and Y. Dedkov, Graphene on metallic surfaces: Problems and perspectives, Phys. Chem. Chem. Phys. **14**, 13502 (2012).

[24] D. Eom, D. Prezzi, K. T. Rim, H. Zhou, M. Lefenfeld, S. Xiao, C. Nuckolls, M. S. Hybertsen, T. F. Heinz, and G. W. Flynn, Structure and electronic properties of graphene nanoislands on Co(0001), Nano Lett. **9**, 2844 (2009).

[25] P. W. Sutter, J.-I. Flege, and E. A. Sutter, Epitaxial graphene on ruthenium, Nat. Mater. **7**, 406 (2008).

[26] Y. S. Park, J. H. Park, H. N. Hwang, T. S. Laishram, K. S. Kim, M. H. Kang, and C. C. Hwang, Quasi-Free-Standing Graphene Monolayer on a Ni Crystal through Spontaneous Na Intercalation, Phys. Rev. X **4**, 031016 (2014).

[27] M. Alattas and U. Schwingenschlögl, Quasi-freestanding graphene on Ni(111) by Cs intercalation, Sci. Rep. **6**, 26753 (2016).

[28] N. Ligato, A. Cupolillo, and L. S. Caputi, Study of the intercalation of graphene on Ni(111) with Cs atoms: Towards the quasi-free graphene, Thin Solid Films **543**, 59 (2013).

[29] M. S. Dresselhaus and G. Dresselhaus, Intercalation compounds of graphite, Adv. Phys. **51**, 1 (1981).

[30] M. Caragiu and S. Finberg, Alkali metal adsorption on graphite: A review, J. Phys. Condens. Matter **17**, R995 (2005).

[31] K. M. Hock and R. E. Palmer, Temperature dependent behaviour in the adsorption of submonolayer potassium on graphite, Surf. Sci. **284**, 349 (1993).

[32] G. Yoon, H. Kim, I. Park, and K. Kang, Conditions for reversible Na intercalation in graphite: Theoretical studies on the interplay among guest ions, solvent, and graphite host, Adv. Energy Mater. **7**, 1601519 (2017).

[33] J. S. Bunch, S. S. Verbridge, J. S. Alden, A. M. Van Der Zande, J. M. Parpia, H. G. Craighead, and P. L. McEuen, Impermeable

atomic membranes from graphene sheets, Nano Lett. **8**, 2458 (2008).

[34] D. W. Boukhvalov and C. Virojanadara, Penetration of alkali atoms throughout a graphene membrane: theoretical modeling, Nanoscale **4**, 1749 (2012).

[35] M. Petrović, I. Šrut Rakić, S. Runte, C. Busse, J. T. Sadowski, P. Lazić, I. Pletikosić, Z.-H. Pan, M. Milun, P. Pervan, N. Atodiresei, R. Brako, D. Šokčević, T. Valla, T. Michely, and M. Kralj, The mechanism of caesium intercalation of graphene, Nat. Commun. **4**, 2772 (2013).

[36] C. S. Praveen, S. Piccinin, and S. Fabris, Adsorption of alkali adatoms on graphene supported by the Au/Ni(111) surface, Phys. Rev. B **92**, 075403 (2015).

[37] J. Halle, N. Néel, and J. Kröger, Filling the gap: Li-intercalated graphene on Ir(111), J. Phys. Chem. C **120**, 5067 (2016).

[38] P. Pervan, P. Lazić, M. Petrović, I. Šrut Rakić, I. Pletikosić, M. Kralj, M. Milun, and T. Valla, Li adsorption versus graphene intercalation on Ir(111): From quenching to restoration of the Ir surface state, Phys. Rev. B **92**, 245415 (2015).

[39] F. Bisti, G. Profeta, H. Vita, M. Donarelli, F. Perrozzi, P. M. Sheverdyaeva, P. Moras, K. Horn, and L. Ottaviano, Electronic and geometric structure of graphene/SiC(0001) decoupled by lithium intercalation, Phys. Rev. B **91**, 245411 (2015).

[40] C. Struzzi, C. S. Praveen, M. Scardamaglia, N. I. Verbitskiy, A. V. Fedorov, M. Weinl, M. Schreck, A. Grüneis, S. Piccinin, S. Fabris, and L. Petaccia, Controlled thermodynamics for tunable electron doping of graphene on Ir(111), Phys. Rev. B **94**, 085427 (2016).

[41] M. Bianchi, E. D. L. Rienks, S. Lizzit, A. Baraldi, R. Balog, L. Hornekær, and P. Hofmann, Electron-phonon coupling in potassium-doped graphene: Angle-resolved photoemission spectroscopy, Phys. Rev. B **81**, 041403 (2010).

[42] A. Nagashima, N. Tejima, and C. Oshima, Electronic states of the pristine and alkali-metal-intercalated monolayer graphite/Ni(111) systems, Phys. Rev. B **50**, 17487 (1994).

[43] M. T. Johnson, H. I. Starnberg, and H. P. Hughes, Electronic structure of alkali metal overlayers on graphite, Surf. Sci. **178**, 290 (1986).

[44] N. R. Gall, E. V. Rut'kov, and A. Ya. Tontegode, Two dimensional graphite films on metals and their intercalation, Int. J. Mod. Phys. **11**, 1865 (1996).

[45] T. Langer, D. F. Förster, C. Busse, T. Michely, H. Pfnür, and C. Tegenkamp, Sheet plasmons in modulated graphene on Ir(111), New J. Phys. **13**, 053006 (2011).

[46] I. Pletikosić, M. Kralj, D. Sokčević, R. Brako, P. Lazić, and P. Pervan, Photoemission and density functional theory study of Ir(111); energy band gap mapping, J. Phys.: Condens. Matter **22**, 135006 (2010).

[47] M. Kralj, I. Pletikosić, M. Petrović, P. Pervan, M. Milun, A. T. N'Diaye, C. Busse, T. Michely, J. Fujii, and I. Vobornik, Graphene on Ir(111) characterized by angle-resolved photoemission, Phys. Rev. B **84**, 075427 (2011).

[48] K. M. Hock, J. C. Barnard, R. E. Palmer, and H. Ishida, Competing Routes for Charge Transfer in Co-Adsorption of K and O_2 on Graphite, Phys. Rev. Lett. **71**, 641 (1993).

[49] P. Hohenberg and W. Kohn, Inhomogeneous electron gas, Phys. Rev. **136**, B864 (1964).

[50] W. Kohn and L. J. Sham, Self-consistent equations including exchange and correlation effects, Phys. Rev. **140**, A1133 (1965).

[51] G. Kresse and J. Hafner, *Ab initio* molecular dynamics for liquid metals, Phys. Rev. B **47**, 558 (1993).

[52] G. Kresse and J. Furthmüller, Efficient iterative schemes for *ab initio* total-energy calculations using a plane-wave basis set, Phys. Rev. B **54**, 11169 (1996).

[53] P. E. Blöchl, Projector augmented-wave method, Phys. Rev. B **50**, 17953 (1994).

[54] G. Kresse and D. Joubert, From ultrasoft pseudopotentials to the projector augmented-wave method, Phys. Rev. B **59**, 1758 (1999).

[55] M. Dion, H. Rydberg, E. Schröder, D. C. Langreth, and B. I. Lundqvist, Van der Waals Density Functional for General Geometries, Phys. Rev. Lett. **92**, 246401 (2004).

[56] J. Klimeš, D. R. Bowler, and A. Michaelides, Van der Waals density functionals applied to solids, Phys. Rev. B **83**, 195131 (2011).

[57] A. D. Becke, Density-functional exchange-energy approximation with correct asymptotic behavior, Phys. Rev. A **38**, 3098 (1988).

[58] H. J. Monkhorst and J. D. Pack, Special points for Brillouin-zone integrations, Phys. Rev. B **13**, 5188 (1976).

[59] G. Makov and M. C. Payne, Periodic boundary conditions in *ab initio* calculations, Phys. Rev. B **51**, 4014 (1995).

[60] J. Neugebauer and M. Scheffler, Adsorbate-substrate and adsorbate-adsorbate interactions of Na and K adlayers on Al(111), Phys. Rev. B **46**, 16067 (1992).

[61] S. Ulstrup, M. Andersen, M. Bianchi, L. Barreto, B. Hammer, L. Hornekær, and P. Hofmann, Sequential oxygen and alkali intercalation of epitaxial graphene on Ir(111): Enhanced many-body effects and formation of pn-interfaces, 2D Mater. **1**, 025002 (2014).

[62] S. Schumacher, T. O. Wehling, P. Lazic, S. Runte, D. F. Forster, C. Busse, M. Petrovic, M. Kralj, S. Blucollectivegel, N. Atodiresei, V. Caciuc, and T. Michely, The backside of graphene: Manipulating adsorption by intercalation, Nano Lett. **13**, 5013 (2013).

[63] K.-H. Jin, S.-M. Choi, and S.-H. Jhi, Crossover in the adsorption properties of alkali metals on graphene, Phys. Rev. B **82**, 033414 (2010).

[64] S. Tsuzuki, M. Yoshida, T. Uchimaru, and M. Mikami, The origin of the cation/π interaction: The significant importance of the induction in Li^+ and Na^+ complexes, J. Phys. Chem. A **105**, 769 (2001).